

The role of the Beaufort Gyre in Arctic climate variability: Seasonal to decadal climate scales

A. Proshutinsky

Physical Oceanography Department, Woods Hole Oceanographic Institution, Woods Hole, Massachusetts, USA

R. H. Bourke

Department of Oceanography, Naval Postgraduate School, Monterey, California, USA

F. A. McLaughlin

Institute of Ocean Sciences, Sidney, British Columbia, Canada

Received 9 July 2002; accepted 8 October 2002; published 5 December 2002.

[1] This paper presents a new hypothesis along with supporting evidence that the Beaufort Gyre (BG) plays a significant role in regulating the Arctic climate variability. We propose and demonstrate that the BG accumulates a significant amount of fresh water (FW) during one climate regime (anticyclonic) and releases this water to the North Atlantic (NA) during another climate regime (cyclonic). This hypothesis can explain the origin of the salinity anomaly (SA) periodically found in the NA as well as its role in the decadal variability in the Arctic region. **INDEX TERMS:** 4207 Oceanography: General: Arctic and Antarctic oceanography; 4215 Oceanography: General: Climate and interannual variability (3309); 4263 Oceanography: General: Ocean prediction; 4255 Oceanography: General: Numerical modeling. **Citation:** Proshutinsky, A., R. H. Bourke, and F. A. McLaughlin, The role of the Beaufort Gyre in Arctic climate variability: Seasonal to decadal climate scales, *Geophys. Res. Lett.*, 29(23), 2100, doi:10.1029/2002GL015847, 2002.

1. Introduction

[2] The present state of the Arctic Ocean and its influence on the global climate system strongly depend on the Arctic Ocean freshwater budget (FB) [Aagaard and Carmack, 1989, hereinafter *A&C*; Carmack, 2000] because fluctuations in the freshwater export may significantly influence the depth and volume of deep water formation in the NA and ultimately the strength of the global thermohaline circulation. The traditional approach for investigations of the FB has been to perform a detailed analysis of its major components including river runoff, the inflow of waters from the Atlantic and Pacific Oceans, the outflows through Fram Strait and the Canadian Archipelago, the atmospheric moisture flux and the annual cycle of ice formation and melt [Lewis, 2000]. Significantly less attention has been paid to the processes involved in the storage of FW in the Arctic Ocean and its temporal variability. The regional differences in this storage (e.g., in ice thickness and in ocean salinity) are substantial [A&C; Carmack, 2000]. For instance, the Canadian Basin contains about 45,000 km³ of FW calculated relative to the salinity 34.80 by A&C. This is 10–15

times larger than the total annual river runoff to the Arctic Ocean, and at least two times larger than the amount of FW stored in the ice. A release of only 5% of this FW is enough to cause a SA in the NA comparable in magnitude to the Great Salinity Anomaly of the 1970s. The largest freshwater storage area is located in the BG, identified by a salinity minimum at depths 5–400 m (Figure 1a–1c.). This anomaly drives the BG geostrophic circulation anticyclonically (Figure 1d). We propose that the FB of the BG and the freshwater flux to the NA depend significantly on the intensity of this SA and climatic conditions conducive to the transport of FW from the BG to the NA. This paper provides a step in understanding the origin of this anomaly and the nature of its variability. Characteristics and sources of the data are presented in Table 1.

2. Beaufort Gyre as a Flywheel

[3] The origin of the salinity minimum in the BG can be inferred by a comparison of the seasonal change in wind and ice motion. Figure 2 shows the wind and ice drift patterns seasonally averaged for 1979–1997. In winter (September–May), the wind (Figure 2a) drives the ice and ocean anticyclonically (Figure 2c) and the ocean accumulates potential energy through a deformation of the salinity field (Ekman convergence and subsequent downwelling, Figure 1c). The strength of the horizontal salinity gradient and resultant geostrophic circulation depend on the intensity and duration of the anticyclonic winds. During winter the wind-driven and geostrophic currents coincide to set up a strong anticyclonic ice rotation (Figure 2c).

[4] In summer (June–August), the wind is weaker or it may even be cyclonic (Figure 2b) but in the mean the ice still rotates anticyclonically (Figure 2d). An obvious conclusion is that in summer the ocean geostrophic circulation prevails and may drive the ice against the wind motion. The SA and freshwater content (FC) in the BG (Figure 1b) must decrease in summer, because without wind support, the ocean loses potential energy, i.e., Ekman pumping is reduced. During the following winter the ocean again accumulates potential energy. Hence, the climatic structure of the salinity and dynamic height distribution remain rather persistent (not shown) although exhibiting some seasonal and interannual variability. The seasonal change in FC in the Canadian Basin is about 7% based on the data from

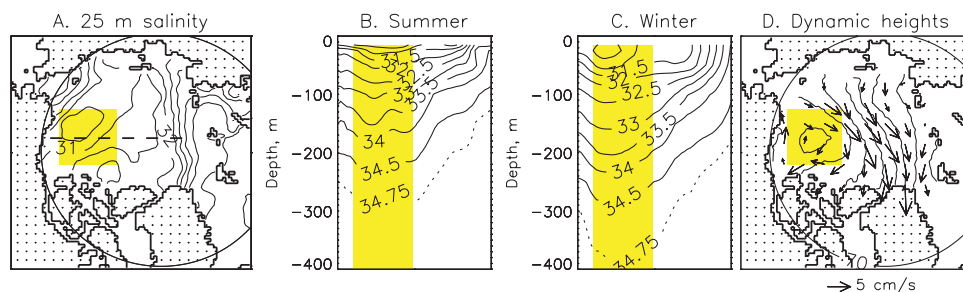


Figure 1. (a) The salinity at 25 m. Contour interval is 0.5. (b), (c) Salinity along dashed line in summer and winter. (d) Dynamic heights relative to 200 db and direction of geostrophic currents. Contour interval is 50 dyn. mm.

EWG atlases. In the 1950s and 1970s, the winter FC was $47,174 \text{ km}^3$ and $44,581 \text{ km}^3$, and the summer FC was $43,949 \text{ km}^3$ and $41,468 \text{ km}^3$, respectively.

[5] When viewed on a seasonal scale, the BG salinity anomaly stabilizes the circulation, remaining essentially anticyclonic throughout the year, thus permitting the BG geostrophic circulation cell to serve as a freshwater flywheel for the Arctic Ocean circulation.

[6] Some modeling results illustrating this mechanism are shown in Figure 3. An idealized situation has been tested using the Princeton Ocean Model in a $2000 \times 2000 \text{ km}$ basin with 1500 m depth. The basin T-S structure was initially horizontally uniform but vertically stratified (similar to climatology), then it was forced for 9 months by symmetric anticyclonic winds (5 m/s) followed by 3 months of cyclonic symmetric winds (3 m/s) similar to climatology presented in Figures 2a–2b. No sources of salt or heat were prescribed. The anticyclonic winds generate downwelling in the central basin and upwelling along the boundaries (Figures 3a–3b). The results after anticyclonic forcing are similar to the winter conditions, and the salinity structure in Figure 3b resembles that in Figure 1c. The addition of cyclonic winds leads to upwelling in the central basin and downwelling along the boundaries and to a reduction in the SA generated by anticyclonic winds (Figures 3c–3d). The circulation pattern in Figure 3c is similar to the ice drift pattern in Figure 2d, i.e., it is still anticyclonic but is weaker than in winter. The salinity distribution in Figure 3d resembles the summer salinity distribution in Figure 1b when the cyclonic wind forcing leads to the release of FW from deep to upper layers. The seasonal variability of the model's FC in the central part of the basin is about 10%, similar to that based on observations. This seasonal mechanism of freshwater accumulation and release is extended to the decadal time scale in the next section.

3. Hypothesis

[7] A hypothetical chain of relationships among atmosphere, ice and ocean in the Arctic at the decadal time scale has been proposed by Mysak and Venegas [1998], Proshutinsky et al. [1999] (hereinafter *P99*) and others but it is important to know what causes the variability. In order to explain the relationship between the wind-driven and geostrophic circulation and their influence on the accumulation and release of FW we examine the interplay between the atmosphere, ice and ocean in terms of the two circulation

regimes identified by Proshutinsky and Johnson [1997] (hereinafter *P&J*).

3.1. ACCR and Transition to CCR

[8] During the anticyclonic circulation regime (ACCR), when high sea level atmospheric pressure (SLP) prevails in the Arctic, the ocean accumulates FW through the increase of FW volume in the BG and through the increase of ice thickness and area due to enhanced ice growth (the Arctic is colder during an ACCR than during a cyclonic circulation regime (CCR) as shown in Proshutinsky 99). Ice is additionally accumulated due to convergence and ridging. River runoff is increased (trajectories of cyclones are shifted toward land, [*P&J*]) and more FW accumulates in the surface waters. When anticyclonic winds are prevalent, the water flow towards Fram Strait is reduced [*P&J*; Tremblay and Mysak, 1998]. Consequently, the ice and water flux from the Arctic Ocean to the Greenland Sea and the transport of Atlantic Water into the Arctic Ocean (as a compensation of outflow) are weaker than usual. Deep convection in the Greenland Sea is then enhanced because the vertical stratification is reduced (less FW in the surface waters). This decoupling of the Greenland, Iceland, and Norwegian Seas (GIN Sea) from the Arctic leads to their eventual warming.

[9] All of the above processes lead (with some time lag) to an increase in the gradient of dynamic height between the BG and the NA. The resultant geostrophic circulation increases as does the outflow of FW and ice from the Arctic. During warming of the GIN Sea, the Icelandic

Table 1. Characteristics of Data

| Parameter | Period Span | Reference Period | Figure | Data Source |
|--------------|-------------|------------------|------------------|--------------------|
| Salinity (S) | 1970–1979 | Winter | Figure 1a and 1c | EWG ^a |
| S | 1970–1979 | Summer | Figure 1b | EWG ^a |
| T, S | 1970–1979 | Jan.–Dec. | Figure 1d | EWG ^a |
| S | 1973–1979 | Mar.–May | Figure 4a | AARI |
| Buoy drift | 1978–1997 | Sept.–May | Figure 2c | IABP ^b |
| Buoy drift | 1978–1997 | Jun.–Aug. | Figure 2d | IABP ^b |
| SLP | 1978–1997 | Sep.–May | Figure 2a | NRA ^c |
| SLP | 1978–1997 | Jun.–Aug. | Figure 2b | NRA ^c |
| SIC | 1978–1997 | Sep.–May | Figure 5a, 5b | NSIDC ^d |

^aEnvironmental Working Group Atlas [1997, 1998].

^bInternational Arctic Buoy Program.

^cNRA - NCAR/NCEP reanalysis; National Center for Environmental Prediction (NCEP); National Center for Atmospheric Research (NCAR).

^dNational Snow and Sea Ice Data Center passive microwave NASA team algorithm).

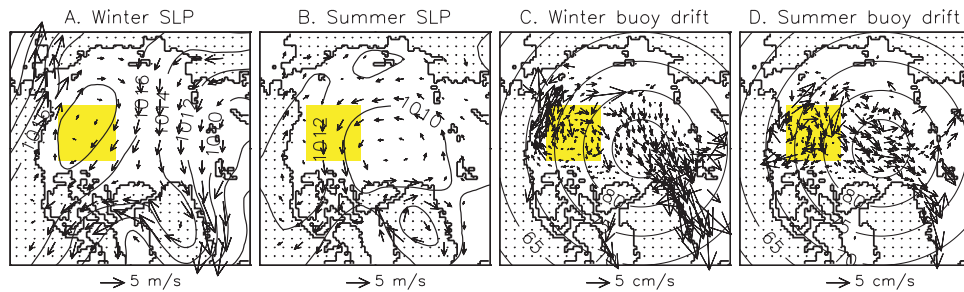


Figure 2. Winter (a) and summer (b) sea level pressure (SLP, hPa) and geostrophic wind. (c),(d) Seasonal ice drift.

Low intensifies and moves to the north leading to an intensification of the transport of Atlantic waters into the Arctic Ocean. This increase in warm water flux to higher latitudes enhances the penetration of atmospheric cyclones into the Arctic, and ultimately decreases the SLP in the Arctic. Warming of the Arctic establishes the CCR.

3.2. CCR and Transition to ACCR

[10] During the CCR, when low SLP prevails in the Arctic (see table characterizing different environmental features of CCR and ACCR in *P&J*), the Arctic Ocean releases FW to the NA through the passages in the Canadian Archipelago and Fram Strait. Warming in the Arctic during the CCR increases ice melting and releases additional FW to the central basin. The accumulation and storage of FW in the BG is not favored by the CCR (even though the cyclonic regime leads to increased ice melt, the FW is not accumulated in the BG because of Ekman divergence and upwelling causing a decrease of freshwater volume in the BG), and hence more FW is available for transport to the NA. River runoff is lower during the CCR than during the ACCR but precipitation over the ocean is increased and hence more FW is available for immediate release to the NA. At the peak of these processes, when all of them coincide, we observe a low SA in the GIN Sea.

[11] After several years of increased release of ice and FW to the GIN Sea, the surface layer becomes cooler and fresher, and the ice extent increases in the Greenland Sea. Freshening associated with melting of the increased ice volume and increased flux of fresher surface waters leads to an increase in stratification and a decrease in the interaction between the deep ocean and the atmosphere; deep water convection is consequently suppressed. After several years the dynamic height gradient between the BG

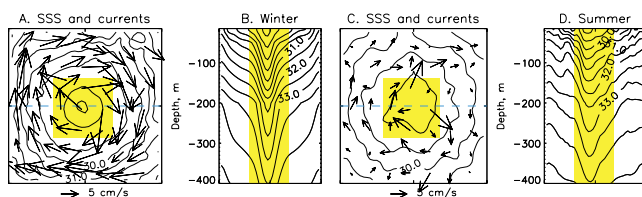


Figure 3. Results of numerical experiments in the ideal basin. Contour interval of salinity is 0.5. (a) Sea surface salinity (SSS) and surface currents. (b) Salinity section along dashed line. Both figures show results after 9 months of anticyclonic symmetric wind forcing. (c), (d) The same characteristics as in (a) and (b), respectively, but after an additional 3 months of symmetric cyclonic wind forcing.

and the NA (and consequently the geostrophic circulation) decreases, the Icelandic Low moves to the south and the interactions between the GIN Sea and the Arctic Ocean become weaker, reestablishing the ACCR. In this sequence of processes the accumulation and release of FW and ice plays a fundamental role in the interaction between the Arctic Basin and the GIN Sea.

4. Discussion and Conclusions

[12] In order to support our hypothesis we have analyzed the variability of the FC in the BG (yellow box in Figures 1 and 2) using 1973–1979 March–May T-S surveys conducted by the Arctic and Antarctic Research Institute (AARI, personal communication). A time series of the FC anomaly for this 7-year period is shown in Figure 4a. Assuming that the FC in the BG depends on the intensity and direction of the wind-driven circulation, we correlated the FC for each year with the annual mean sea surface height gradient (SSHG) in the BG obtained from a 2-D barotropic wind-driven coupled ice-ocean model run results [*P&J, P99*]. This SSHG is an integrating parameter that reflects the intensity of the barotropic wind-driven circulation over the Arctic. When the SSHG is positive, the ACCR prevails over the Arctic; conversely for CCR years. The time series of SSHG anomaly for 1973–1979 (departure of SSHG from its mean for 1973–1979) is shown in Figure 4a. The correlation

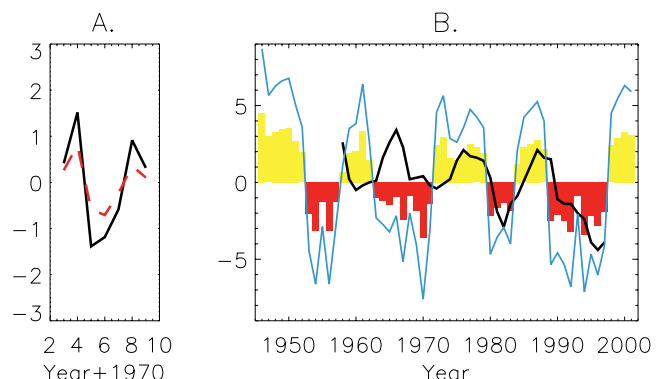


Figure 4. (a) The FC anomaly (solid blue line) from observations and SSHG (red dashed line). (b) The FC anomaly (solid blue line) from reconstruction and SSHG (red and yellow bars) as defined by *P&J*. The thick black line depicts the sea ice volume (km^3/year) anomalies from *Hilmer and Lemke* [2001]. Vertical axes show units of SSHG ($\times 10^{-6}$), sea ice volume anomalies (km^3/year), and the FC anomalies (km^3/year).

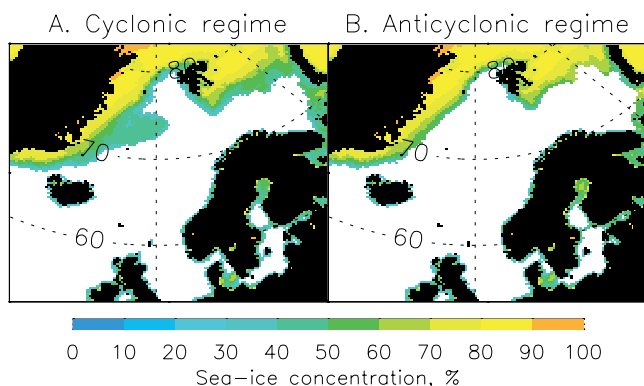


Figure 5. Sea ice concentration in the GIN Sea averaged for the two CCRs: 1980–1983 and 1989–1997 (a), and two ACCRs: 1984–1988 and 1998–2000 (b).

between the FC and SSHG anomalies is 0.89. In order to expand this rather short time series to a longer period, we employed a proportional relationship obtained by linear regression (the FC anomaly = $2. \times$ SSHG anomaly) to reconstruct the anomaly of the FC in the BG for 1946–2001 (Figure 4b). The difference between the FC during ACCR and CCR in the yellow box area is about $10^4 \text{ km}^3/\text{year}$, which is about 3 times larger than the annual freshwater input from river runoff estimated by A&C as $3300 \text{ km}^3/\text{year}$. This suggests that the FW released from the BG during CCRs can be significantly more important than that from all other freshwater sources.

[13] Another component of the FC is the volume of ice. No direct observations are available but we can use some results from modeling studies. Figure 4b shows the anomaly of ice volume based upon the model studies by Hilmer and Lemke [2001]. This simulation reveals a pronounced decadal variability of the ice volume which is in agreement with the SSHG (except before 1970). In concert with our previous discussion, the volume of ice increases during ACCRs and decreases during CCRs. The disagreement noted for years prior to 1970 could be explained by a lack of good SLP data prior to introduction of the IABP.

[14] Another confirmation of different rates of FW release from the Arctic is the ice extent in the GIN Sea. Figure 5 shows the sea ice concentration (SIC) averaged for the ACCR and CCR years since 1978 (see Table). An enhanced development of ice extending NW into the Greenland Sea is noted during CCRs (Figure 5a). This provides indirect evidence that deep convection is suppressed during CCRs because of the large volume of FW in the surface layer of the Greenland Sea.

[15] One may wonder how the SA in the BG may change in response to climate change. Recent observations show that the climatologically stable ACCR, dominant during the 1980s, has been replaced by a CCR starting about 1989. As a result, for most of the past decade the intensity of the Arctic High has decreased and the summer cyclonic circulation period

(Figure 2b) has commenced earlier and lasted longer than usual. These conditions must necessarily lead to a salinity increase in the deeper layers of the BG (upwelling in response to the cyclonic forcing, similar to Figures 1b and 3c–3d), a reduction in the speed of the geostrophic current and to a decrease of salinity in the upper layers of the BG. As a result, the FW stored in the upper layers of the BG becomes available for output to the NA through increased transport by the cyclonic wind-driven circulation. Physical and geochemical data collected between 1989 and 1995 by McLaughlin *et al.* [2002] reveal that the FC in the Canada Basin has been significantly reduced which confirms the reconstruction results of FC for 1990–1997 (Figure 4b). Since 1997, evidence suggests that a new anticyclonic circulation regime has developed (Figure 4b) and we expect to observe an increase of the FC in the BG.

[16] A substantial release of the BG FW to the NA in response to changing climate conditions can be a source for a large scale SA in the NA, and consequently, a source for an abrupt cooling [A&C; Delworth *et al.*, 1997]. The above perspectives lead us to the conclusion that it is extremely important to understand the structure of the BG water properties, its currents, and their variability in space and time.

[17] **Acknowledgments.** This research has been supported by a grant from NOAA. It is contribution 10756 of the Woods Hole Oceanographic Institution.

References

- Aagaard, K., and E. C. Carmack, The role of sea ice and fresh water in the Arctic circulation, *J. Geophys. Res.*, *94*, 14,485–14,498, 1989.
- Carmack, E. C., The Arctic Ocean's freshwater budget: Sources, storage and export, in *The freshwater budget of the Arctic Ocean*, NATO Science Series, edited by E. L. Lewis, Kluwer Academic Press, 91–126, 2000.
- Delworth, T., S. Manabe, and R. J. Stouffer, Multidecadal climate variability in the Greenland Sea and surrounding regions: A coupled model simulation, *Geophys. Res. Lett.*, *24*, 257–260, 1997.
- EWG (Environmental Working Group), Joint U.S.-Russian Atlas of the Arctic Ocean (CD-ROM). National Snow and Ice Data Center, Boulder, Colorado, 1997, 1998.
- Hilmer, M., and P. Lemke, On the decrease of Arctic sea ice volume, *Geophys. Res. Lett.*, *27*(22), 3751–3754, 2001.
- Lewis, E. L., (ed.), *The freshwater budget of the Arctic Ocean*, NATO Science Series, Kluwer Academic Publishers, 623 p., 2000.
- McLaughlin, F., E. Carmack, R. W. MacDonald, A. J. Weaver, and J. Smith, The Canada Basin 1989–1995: Upstream events and far-field effects of the Barents Sea, *J. Geophys. Res.*, *107*(C7), 10.1029/2001JC000904, 2002.
- Mysak, L. A., and S. A. Venegas, Decadal climate oscillations in the Arctic: A new feedback loop for atmosphere-ice-ocean interactions, *Geophys. Res. Lett.*, *25*(19), 3607–3610, 1998.
- Proshutinsky, A. Y., and M. A. Johnson, Two circulation regimes of the wind-driven Arctic Ocean, *J. Geophys. Res.*, *102*, 12,493–12,514, 1997.
- Proshutinsky, A., I. V. Polyakov, and M. A. Johnson, Climate states and variability of Arctic ice and water dynamics during 1946–1997, *Polar Research*, *18*(2), 135–142, 1999.
- Tremblay, L. B., and L. A. Mysak, On the origin and evolution of sea-ice anomalies in the Beaufort-Chukchi Sea, *Climate Dynamics*, *14*, 451–460, 1998.

A. Proshutinsky Physical Oceanography Department, Woods Hole Oceanographic Institution, MS # 29,360 Woods Hole Road, Woods Hole, MA 02543, USA. (aproshutinsky@whoi.edu)